Optimisation of nonlinear controllers for a quadrotor using metaheuristic algorithm

Nadia Samantha Zuñiga-Peña[1], Norberto Hernández-Romero[1], Juan Carlos Seck-Tuoh-Mora[1], Joselito Medina-Marin[1], Julio Cesar Ramos-Fernández[2]

[1]Área Académica de Ingeniería, Instituto de Ciencias Básicas e Ingeniería, Universidad Autónoma del Estado de Hidalgo, Mineral de la Reforma, México
[2]Departamento de Mecatrónica, Universidad Politécnica de Pachuca, Zempoala, México.

ABSTRACT

Unmanned aerial vehicles (UAVs) facilitate complex activities and are widely used for aerial transport. Quadrotor UAVs (QUAV), the most popular UAV containing four motors, are characterised by higher control properties since they have fewer actuators than degrees of freedom, implying a nonlinear underactuated system. In addition, the coupling of dynamics, flaws while modelling and parameter uncertainty are the factors that hinder the design and implementation of a controller. Here, we present the modelling, optimisation, simulation, and implementation methodology for controllers, proportional-integral-derivative (PID), and super-twisting-sliding mode control (ST-SMC). We carry out the parameterisation problem of controllers using the hunger game search (HGS) metaheuristic algorithm. This process was developed offline, and the values obtained were successfully implemented in simulation and experimental form. The testing platform comprises a motion capture system, Vicon® Bonita cameras, linked by ROS, that allows the known position and the attitude of a Parrot® QUAV bebop1. The whole six dynamics of the QUAV are included in the implementation, translational trajectories X-Y are trapezoidal, and the altitude trajectory is a ramp. The results enabled the comparison of the statistics calculation of each controller. Successful tracking trajectories were obtained even with disturbance when the ST-SMC algorithm was implemented with root mean square error (RMSE)=0.0176.

Corresponding Author:

Norberto Hernández-Romero
Área Académica de Ingeniería, Instituto de Ciencias Básicas e Ingeniería
Universidad Autónoma del Estado de Hidalgo, Mineral de la Reforma
Hidalgo, México
Email: nhromero@uaeh.edu.mx

1. INTRODUCTION

Currently, a wide variety of tasks are performed by unmanned aerial vehicles (UAVs), commonly known as drones. UAVs facilitate complex activities and have extraordinary flexibility in flight mode and advanced features and functionalities such as inspection, agricultural monitoring, rescue operations, collecting different data types, photography, delivery, mapping, and even reforestation efforts [1]. UAVs are also known as cyber-physical systems (CPSs) that integrate computational and physical capabilities. Those attributes allow them to interact with other CPS and humans in real-time [2]. UAVs can contain one to eight rotors; the most common UAV is the four-rotor drone (QUAV). The expansion of technological applications and the reliability of

QUAVs will depend on the success of overcoming challenges associated with control. QUAV issues stem from: i) being underactuated where the number of rotors is lower than the possible movements, ii) its nonlinear nature makes the output change not proportional to the input change, iii) interconnected dynamics cause any change in attitude dynamic to affect a translation dynamic and vice versa, and iv) being chaotic triggers unpredictable and irregular behaviours with minor changes in initial conditions. The complexity of these features presents a challenge when modelling and enhancing controller designs. Ensuring the stability and robustness of QUAVs during flight requires special attention.

Besides the problematic characteristics of the QUAV mentioned above, a discrepancy usually exists between the real system and the dynamic model while designing a controller. These differences correspond to many reasons, for example, external disturbances, unknown parameters, and unmodeled dynamics. Thus, developing comprehensive controllers to track the system along the desired trajectories with minimal deviation is crucial. Presently, QUAV research focuses primarily on refining and developing control algorithms, with a significant emphasis on managing some of the total dynamics control of QUAVs [3]–[5]; on the contrary, we are dealing with the full dynamics, three translational, and three rotational. Novel solutions will further push to apply controllers capable of counteracting and compensating for nonlinearities and chaotic behaviour [6].

These approaches guarantee to reach the goal in the presence of model inaccuracies or uncertainties that may affect the performance of QUAV. In the literature can be found that the development of robust control techniques allows adaptive like [7], an adaptive proportional integral derivative deep feedforward neural network (APIDDFN) is proposed and compared to an optimised APIDDFN in simulations to stabilise the QUAV in response to step signals. The results present fast convergence even in the presence of external disturbance. In predictive, can be found [8], a model predictive controller who anticipates the trajectories by the a priori knowledge of the future reference signals, this work is implemented in simulations. Some backstepping techniques are implemented to stabilise the movements of QUAV as [9], where results show trajectory tracking with significant error in real experiments. Also, optimal backstepping can be found, where parameters are selected using a metaheuristic algorithm to stabilise the dynamics of a QUAV presenting good tracking response in simulations [10]. Combined techniques as nonlinear H_∞ and an observer as presented in [11]. This approach has been implemented for the attitude control. Simulation results demonstrate attenuated disturbance and parametric uncertainty. Sliding mode methods (SMC) are also attractive in the QUAV control problem. SMC strategy has demonstrated effectiveness in rejecting disturbances and uncertainty. Nguyen *et al.* [12] and Huang *et al.* [13] report results in real-time experiments with minor errors in constant reference tracking. Mehmood *et al.* [14], the formation and trajectory of multiple vehicles are controlled using adaptive sliding modes control. The controller is implemented in simulations in the presence of wind disturbance.

The control law of SMC conducts dynamics to a specific surface of the state space, also called the sliding surface. Once the state is on the sliding surface, it remains on. The performance of an SMC has been analyzed, which makes any linear or non-linear system unresponsive to parametric uncertainty and external disturbances [15]. Several variations of SMC have been proposed; for example, a combination of a nonsingular modified controller with a high-order sliding mode observer to enable vehicle trajectory tracking [16]. Adaptable controls with SMC have been implemented to compensate for external disturbances such as wind, which can mainly affect the translational dynamics [17]. In addition, comparisons with robust controllers are developed in experimental platforms [18]. SMC provides robustness to disturbances and unmodeled parameters. However, it is a first-order structure with the disadvantage of chattering when frequency changes. The super-twisting sliding mode model (ST-SMC) has offered an attenuated chattering effect to overcome these limitations. It contains a discontinuous function with an integral term reaching an equilibrium point [15], [19], which results in remarkable differences and benefits among ST-SMC and SMC [20].

The design and implementation of control laws in QUAVs consider multiple parameters or gains that have to be tuned. These parameters must be selected carefully to ensure asymptotic convergence and achieve the desired performance. This parameterization process is critical because a wrong selection of parameters will result in bad performance or an unstable system. In this work, the parameters have been obtained using the population-based metaheuristic algorithm, hunger game search (HGS), applied to an ST-SMC controller to increase robustness. Those metaheuristic methods encompass collaboration capabilities, social interaction, and sharing knowledge and have been demonstrated to enable the solving of multi-objective optimization problems. The literature can include genetic algorithm (MGA-SMC), particle swarm optimization (PSO-SMC), and differential evolution algorithm (DE-SMC), to name a few [21]–[23]. Some researchers have even developed simulations to address the tracking trajectories in QUAVs [24], [25]; in contrast to this work, we are imple-

menting them in simulations and real platforms. Summarizing the above, in most previous works, the whole dynamics need to be considered; some need to be implemented on a real platform, and disturbances to which the QUAV are subjected are not considered. In this sense, the main innovations of this work are outline in:

− Offline optimization of PID and ST-SMC controls was carried out with 18 parameters for each controller. It uses the QUAV nonlinear model for a trajectory with abrupt changes in the presence of disturbances by applying the HGS metaheuristic algorithm.
− Control of translation, altitude and orientation was designed to guarantee asymptotic stability in the sense of Lyapunov.
− The PID and ST-SMC controls are implemented in real-time for the Parrot Bebop1 ®QUAV with the ROS platform and a Vicon positioning system that validates the offline tuning of the controllers by the HGS algorithm.
− It compares the performance of PID controllers and the ST-SMC for tracking trajectory in 3 dimensions. The comparison was developed in simulation and experimental tests, including the complete dynamics of the QUAV.

The paper is organised into six sections. In section 2, the mathematical model of QUAV is shown. In section 3, the proposed structure for implementing ST-SMC control is introduced. In section 4, the process for the optimisation method is detailed. An explanation of the HGS algorithm is included, and the stability test is developed to guarantee dynamics convergence. In section 5, the results of simulations, experiments, and discussion are reported to validate the proposed methodology. Finally, conclusions are presented in section 6.

2. MATHEMATICAL MODEL

The mathematical model of QUAV as shown in Figure 1 is obtained using the Newton-Euler formulation. We offer the translational and attitude dynamics in (1); this system of equations describes the six degrees of freedom of the vehicle: x, y, z, roll, pitch, and yaw, in these order. The system's nonlinearity and dynamics coupling is evident when observing the equations. Translation equations (x, y, z) expose the dependence between attitude and each linear dynamic. In addition, (1) shows the characteristic of being underactuated when we can find only four control signals for the whole six dynamics. In the previous work [26], the procedure was described in detail, explaining the derivation of the model.
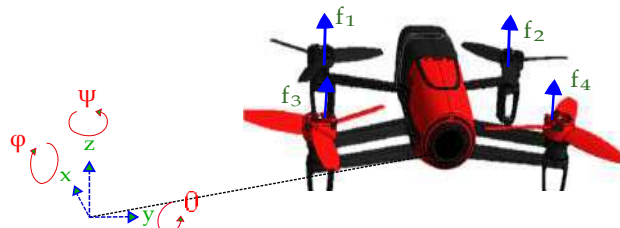

Figure 1. QUAV Parrot bebop 1

$$\ddot{x} = \frac{1}{m}\left(\cos(\psi)\sin(\theta)\cos(\phi) + \sin(\phi)\sin(\psi)\right)u_1 - \frac{k_1}{m}\dot{x}$$

$$\ddot{y} = \frac{1}{m}\left(\sin(\psi)\sin(\theta)\cos(\phi) - \sin(\phi)\cos(\psi)\right)u_1 - \frac{k_2}{m}\dot{y}$$

$$\ddot{z} = \frac{1}{m}(\cos(\phi)\cos(\theta))u_1 - g - \frac{k_3}{m}\dot{z}$$

$$\ddot{\phi} = \frac{(Iy - Iz)}{Ix}\dot{\theta}\dot{\psi} - \frac{k_4}{I_x}\dot{\phi}^2 + \frac{1}{I_x}u_2$$

$$\ddot{\theta} = \frac{(Iz - Ix)}{Iy}\dot{\phi}\dot{\psi} - \frac{k_5}{I_y}\dot{\theta}^2 + \frac{1}{I_y}u_3$$

$$\ddot{\psi} = \frac{(Ix - Iy)}{Iz}\dot{\phi}\dot{\theta} - \frac{k_6}{I_z}\dot{\psi}^2 + \frac{1}{I_z}u_4$$

(1)

3.   CONTROL STRATEGY: ST-SMC

The following structure is proposed to implement the ST-SMC algorithm; first, we have the desired trajectory in every axis *x, y, z* and attitude *yaw*. The desired trajectory is introduced to translational and attitude controllers. The translational controller computes control signal u_1, and simultaneously as desired angles, which, together with ψ_d, are references to the attitude controller. The signals u_2, u_3 and u_4 are computed in attitude controller. In addition to control signals, disturbances are affecting the performance of QUAV, as we can see in Figure 2. Finally, the dynamics of QUAV are again feedback into controllers until the desired path is completed.
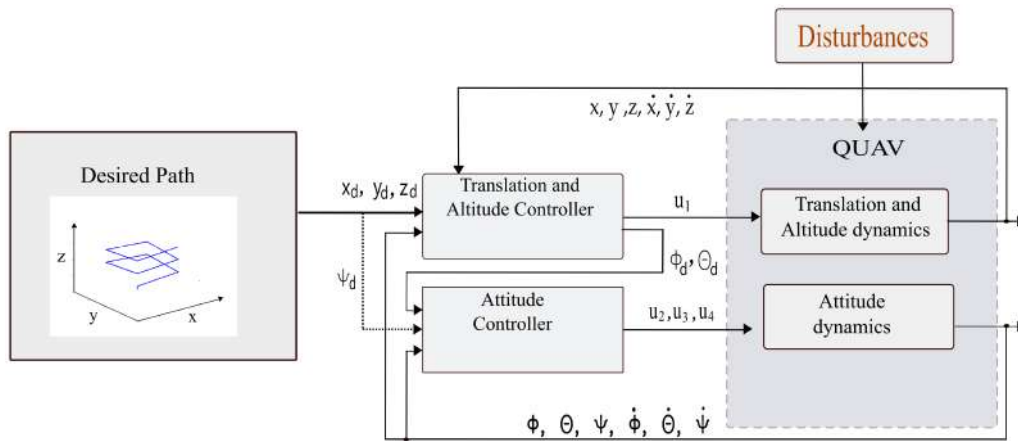
Figure 2. Proposed control strategy

The ST-SMC control design assumes that each dynamic is represented as:

$$\ddot{\chi} = f(\boldsymbol{\chi}) + g(\boldsymbol{\chi})u + w(t) \tag{2}$$

where $f(\boldsymbol{\chi})$ and $g(\boldsymbol{\chi}) \neq 0$ are nonlinear functions of no modelled physics parameters and aerodynamic forces of QUAV, which can be partially or entirely unknown, $\boldsymbol{\chi} = [\chi, \dot{\chi}]$, u is the control signal and $w(t)$ represent external disturbances and unknown parameters.

The sliding surface is defined by:

$$s = \dot{e} + \beta e \tag{3}$$

where e y $\dot{e}$ are the tracking error ($e = \chi_d - \chi$) and its derivative, β, is the convergence rate parameter, choosing $\beta > 0$, we can guarantee that the error tends to zero when time tends to infinity [27]. Deriving (3), is obtained as:

$$\dot{s} = \ddot{e} + \beta\dot{e} = \ddot{\chi}_d - \ddot{\chi} + \beta\dot{e} \tag{4}$$

substituting (2) in (4) we obtain (5).

$$\dot{s} = \ddot{\chi}_d - [f(\boldsymbol{\chi}) + g(\boldsymbol{\chi})u + w(t)] + \beta\dot{e} \tag{5}$$

The control law is composed of two terms, which are a proposed equivalent control signal (u_{eq}) and the sliding control signal (ust) [28];

$$u = u_{eq} + u_{st} \tag{6}$$

where:

$$u_{eq} = \ddot{\chi}_d - [f(\boldsymbol{\chi}) + g(\boldsymbol{\chi})u + w(t)] + \beta\dot{e}$$

$$u_{st} = k_1\sqrt{|s|}sign(s) + k_2\int sign(s)dt.$$

3.1. Translational and altitude control
Altitude dynamic showed in (1) can be represented as (2).

$$\ddot{z} = \frac{1}{m}(\cos\phi\cos\theta)u_1 - \frac{k_3}{m}\dot{z} - g \tag{7}$$

Thus, we can design the control law, in the same manner, to (6), obtaining:

$$u_1 = \frac{m}{\cos\theta\cos\phi}\left(\ddot{z}_d + \beta_z\dot{e}_z + k_1\sqrt{|s_z|}sign(s_z) + k_2\int sign(s_z)dt + w(t)\right) + g \tag{8}$$

here, the equation (8) applies to $-\pi/2 < \phi < \pi/2$ and $-\pi/2 < \theta < \pi/2$

As the following dynamic, translation in the X axis, we have to choose the virtual control signal $\mu_x = \cos\phi\sin\theta\cos\psi + \sin\phi\sin\psi$, resulting in:

$$m\ddot{x} = f(\mathbf{x}) + \mu_x u_1 \tag{9}$$

with control law as in (6).

$$\mu_x = \frac{m}{u_1}\left(\ddot{x}_d + \beta_x\dot{e}_x + k_1\sqrt{|s_x|}sign(s_x) + k_2\int sign(s_x)dt + w(t)\right) \tag{10}$$

In the same way, for the dynamic of Y axis, the virtual control signal is $\mu_y = \cos\phi\sin\theta\sin\psi - \sin\phi\cos\psi$, resulting in (11):

$$m\ddot{y} = \frac{k_2}{m}\dot{y} + \mu_y u_1 \tag{11}$$

with control law in the same way to (6):

$$\mu_y = \frac{m}{u_1}\left(\ddot{y}_d + \beta_y\dot{e}_y + k_1\sqrt{|s_y|}sign(s_y) + k_2\int sign(s_y)dt + w(t)\right) \tag{12}$$

where expressions (10) and (12) are only valid if $u_1 > 0$, which is true as u_1 is the thrust of rotors in the vehicle. With virtual control signals μ_x y μ_y, we can compute the desired angles for attitude control *roll* and *pitch* as (13).

$$\begin{bmatrix} \cos\phi\sin\theta \\ \sin\phi \end{bmatrix} = \begin{bmatrix} \cos\psi & \sin\psi \\ \sin\psi & -\cos\psi \end{bmatrix} \begin{bmatrix} \mu_x \\ \mu_y \end{bmatrix}$$

$$\phi_d = asin(\sin\psi\mu_x - \cos\psi\mu_y)$$
$$\theta_d = asin\left(\frac{\cos\psi\mu_x + \sin\psi\mu_y}{\cos\phi}\right) \tag{13}$$

3.2. Attitude control
The attitude dynamics can be represented as (2), then we can design as in (6).
To *roll* movement, correspond the signal control u_2 as (14).

$$u_2 = I_x\left(\ddot{\phi}_d + \beta_\phi\dot{e}_\phi + k_1\sqrt{|s_\phi|}sign(s_\phi) + k_2\int sign(s_\phi)dt - \frac{(Iy - Iz)}{Ix}\dot{\theta}\dot{\psi}\right) \tag{14}$$

Using the same step for the *pitch* dynamic, control law u_3 can be formulated as (15).

$$u_3 = I_y\left(\ddot{\theta}_d + \beta_\theta\dot{e}_\theta + k_1\sqrt{|s_\theta|}sign(s_\theta) + k_2\int sign(s_\theta)dt - \frac{(Iz - Ix)}{Iy}\dot{\phi}\dot{\psi}\right) \tag{15}$$

Finally, *yaw* movement is controlled by u_4 (16).

$$u_4 = I_z\left(\ddot{\psi}_d + \beta_\psi\dot{e}_\psi + k_1\sqrt{|s_\psi|}sign(s_\psi) + k_2\int sign(s_\psi)dt - \frac{(Ix - Iy)}{Iz}\dot{\theta}\dot{\psi}\right) \tag{16}$$

4.   PARAMETRIC OPTIMIZATION METHOD

Optimization of the ST-SMC controller is performed using the HGS metaheuristic algorithm. The animals' selective behaviour, feeding decisions, and actions inspire the HGS algorithm. The HGS is designed and employs an adaptive weight to simulate the effect of hunger at each search step. Then, the rules most animals follow when facing and adapting to increase the chances of getting food and surviving (games) are modelled. Hunger games have two main phases: the approach to food and the role of hunger in motivating an exhaustive search [29]. Figure 3 shows the sequence in which the HGS algorithm calculates each action based on the need for food for optimisation. We can highlight that after initialising the parameters and calculating the positions or possible solutions, the algorithm verifies in each iteration that the values are within the limits of the search space to delimit it.
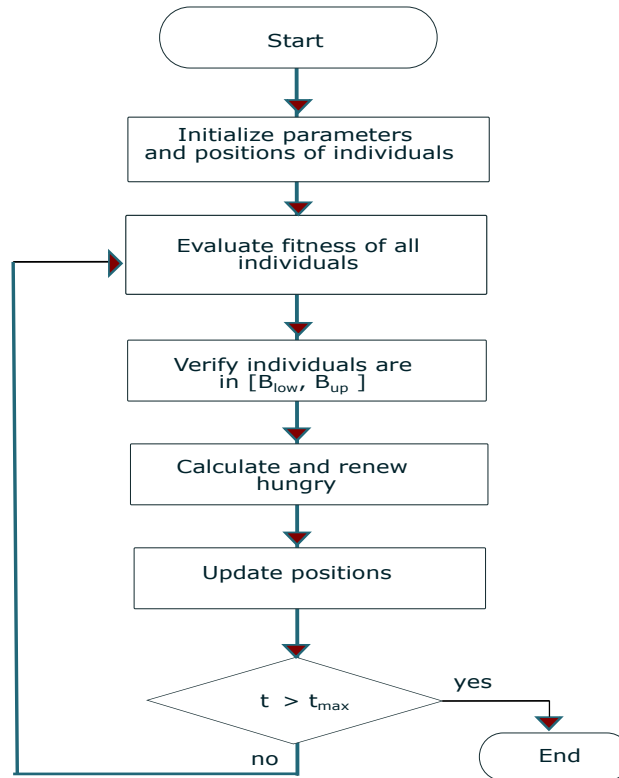
Figure 3. Diagram of HGS optimisation process

The process of HGS starts with an aleatory generation of the possible solutions or population and the eighteen parameters of ST-SMC, formed by three members for each dynamic of the QUAV:

$$P = \{\beta_x \ k_{1_x} \ k_{2_x} \ \beta_y \ k_{1_y} \ k_{2_y} \ \beta_z \ k_{1_z} \ k_{2_z} \ \beta_\phi k_{1_\phi} \ k_{2_\phi} \ \beta_\theta \ k_{1_\theta} \ k_{2_\theta} \ \beta_\psi \ k_{1_\psi} \ k_{2_\psi}\} \qquad (17)$$

where the search of each individual is in space $S = [0, 10]$, the parameters delivered by HGS are introduced to the controller, which in turn computes the control signals for the QUAV. Then, to evaluate the performance of each dynamic, the error between the desired and real trajectory is measured using the mean square error:

$$RMSE = \sqrt{\frac{1}{N} \sum_{i=1}^{G} \sum_{K=0}^{N} (\chi_d^i(k) - \chi^i(k))^2} \qquad (18)$$

where RMSE shows in (18) is the cost function and determines the direction of search of the HGS algorithm. The cycle is repeated until the number of iterations set out is reached. The process can be seen in Figure 4. The variables used to implement HGS are 50 individuals, 20 iterations, and 30 repetitions for both PID and ST-SMC.

In Figure 5, we can observe PID and ST-SMC behaviour during optimisation and show the minimal values reached in every iteration of the HGS algorithm. In Figure 5(a), the fast convergence for PID and in Figure 5(b), a slower convergence that reaches the smallest values while minimising error with the ST-SMC algorithm can be observed. In Table 1, the evaluation of the performance of PID and ST-SMC is reported through a statistic: the best, the mean, the standard deviation, and the worst values obtained while the HGS algorithm was applied.
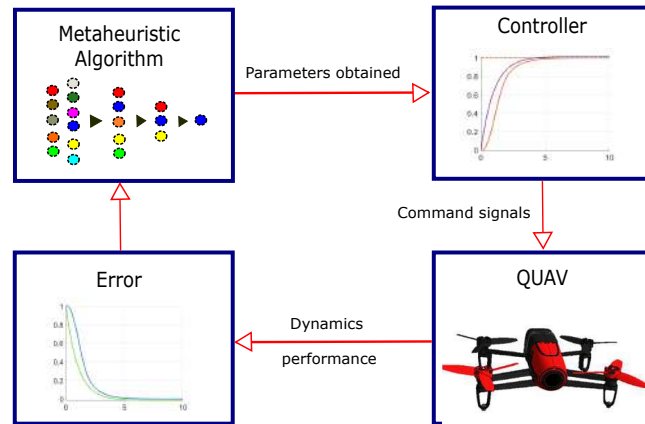
Figure 4. Parametric optimization method for ST-SMC

(a)

(b)
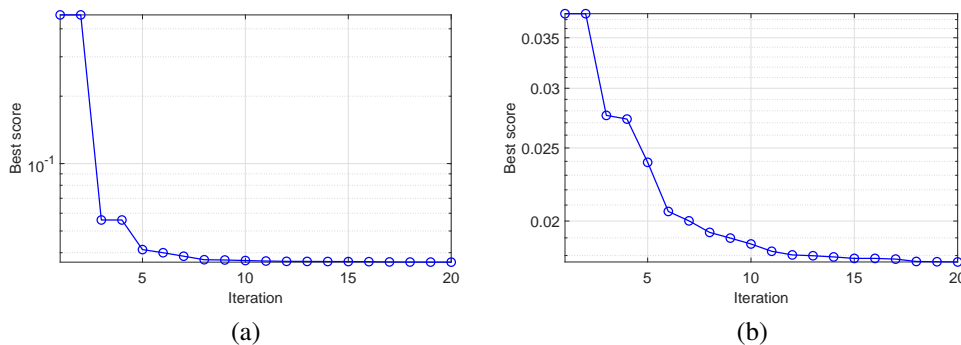
Figure 5. Convergence curves obtained with HGS, 20 iterations, 50 individuals and 30 repetitions (a) the minimum values of RMSE while optimising PID and (b) the minimum values of RMSE while optimising ST-SMC

Table 1. Experimental results of RMSE with 50 individuals, 20 evolutions, and 30 repetitions

Statistics	PID	ST-SMC
Best	0.036290839363412	0.017650649172323
Mean	0.627945953121468	0.018197329174221
SD	0.623996714866044	0.000564758140820
Worst	1.620029205574020	0.020239081645909

4.1. Stability test

For each dynamic, setting conditions that ensure the system's stability is possible. For the dynamics of Z, shown in (7), the stability is determined by *Theorem1* and is tested with Lyapunov's sense analysis. *Theorem 1.* Suppose for the system of (7) the derivative of the perturbation ω is globally bounded $|\dot{\omega}| \leq \omega_1$ with $\omega > 0$, and the gains k_1 and k_2 are chosen as:

$$k_1 > 0, \qquad k_2 > 2k_1\omega + 4\left(\frac{\omega^2}{k_1^2}\right) \tag{19}$$

then, the control law proposed in (8) will bring the dynamics to the slip surface $s = 0$, and the tracking error and its derivative will asymptotically converge to zero. The theorem determines the conditions the gains k_1 and k_2 must satisfy. This process is detailed in [30], and the analysis can be further explained in [31]. Substituting the values obtained by the HGS algorithm for the dynamics of Z and the value of the perturbation $\omega = \frac{1}{2}cos(t)$, with $k_1 = 1.223$, the value of $k_2 > 1.891$. It is observed that the condition is satisfied so that the convergence of the tracking errors to zero and the convergence of the dynamics to the slip surface can be ensured. The same procedure is performed for each of the dynamics. However, for space reasons, they are not included in this work.

5.   RESULTS AND DISCUSSION

This section is divided into two parts: the results obtained from numerical simulations and the experimental results implemented in a physical platform. In both implementations, the dynamic performance of QUAV is evaluated. First, without disturbances and then with a disturbance added to validate the execution of trajectory tracking.

5.1.   Simulation results

The dynamic model (1) is implemented through simulations to validate the behaviour of QUAV when the ST-SMC is applied. A comparison with an optimized PID is developed to compare the robustness of optimized ST-SMC. Calculations were performed in a Mac OS Big Sur (Intel core i9, RAM 24 GB, and 1 TB hard disk), using MATLAB 2015a (MathWorks) for each algorithm. The gain parameters for each algorithm are shown in Table 2. The physical parameters in (1), used for the implementation in simulations, can be found in Table 3 obtained from [32]. The parameters to optimize the PID controller are:

$$P = \{k_{p_x} k_{i_x} k_{d_x} k_{p_y} k_{i_y} k_{d_y} k_{p_z} k_{i_z} k_{d_z} k_{p_\phi} k_{i_\phi} k_{d_\phi} k_{p_\theta} k_{i_\theta} k_{d_\theta} k_{p_\psi} k_{i_\psi} k_{d_\psi}\} \qquad (20)$$

the desired trajectories are trapezoidal for translational (X and Y) and a ramp for altitude dynamic (Z) and attitude (ψ).

Table 2. Parameters obtained by HGS

| Dynamic | Algorithm | | | |
| | PID | | ST-SMC | |
	Parameter	Value	Parameter	Value
x	k_p	9.999	β	2.0
	k_i	4.319	k_1	2.0
	k_d	9.144	k_2	1.997
y	k_p	10.0	β	2.0
	k_i	4.215	k_1	2.0
	k_d	10.0	k_2	1.999
z	k_p	9.99	β	1.401
	k_i	10.0	k_1	1.223
	k_d	0	k_2	1.898
ϕ	k_p	9.882	β	0.066
	k_i	4.386	k_1	0.0469.
	k_d	0	k_2	1.9846
θ	k_p	4.618	β	0.075
	k_i	0	k_1	0.039
	k_d	0	k_2	2.0
ψ	k_p	10.0	β	0.089
	k_i	0.701	k_1	0.005
	k_d	1.029	k_2	0.005

Table 3. Parameters implemented in simulation

Parameter	Value	Units
Mass	0.4	kg
Moment of inertia	$I_x = 0.000906 I_y = 0.001242, I_z = 0.002054$	kgm^2
Translational drag coefficient	$k_{1,2,3} = 5.56x10^{-04}$	$--$
Coefficient of aerodynamic friction	$k_{4,5,6} = 0.3729$	$--$
Acceleration of gravity	9.81	m/s^2

5.1.1. Comparison PID-ST-SMC

In this section, the evaluation of the strategy of the ST-SMC algorithm detailed in section 3, and the optimised PID, which is further explained in [26], is developed. Both algorithms are optimized using HGS algorithm and tested on trajectory tracking of a QUAV. That comparison is feasible because each algorithm has 18 parameters to optimize and a similar structure. The experiments were developed without the presence of disturbances. Results show that both algorithms track the QUAV to the desired trajectory. However, the PID experiment presents a significant error compared with the ST-SMC response. In Figure 6, we can observe the performance of QUAV when both algorithms are implemented. Figure 6(a) show the result of the simulation of the PID controller. It can be seen the three-dimensional trajectory with an overshot in the X and Y axis when the changes of direction exist. On the other hand, Figure 6(b) show a trajectory with minimal overshoot and no oscillation when ST-SMC control is implemented. Even when the changes of direction exist, the X and Y axis presents the smallest error compared with PID controller.

| (a) | (b) |
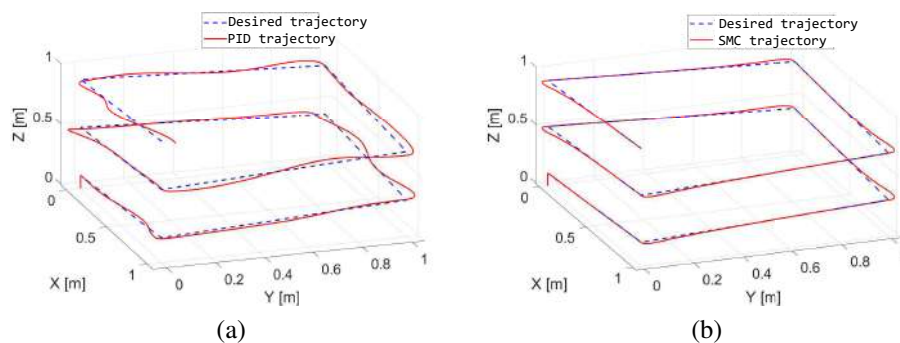
Figure 6. Simulations of trajectory tracking applying PID and ST-SMC control algorithms without a disturbance (a) QUAV performance in X-Y-Z axis with PID control and (b) QUAV performance in X-Y-Z axis with TC-SMC control

5.1.2. Comparison of tracking performance: PID and ST-SMC controllers adding a disturbance

To validate the performance of the proposed ST-SMC under external disturbances, we introduced a disturbance signal $\omega = \frac{1}{2}\cos t$, in the same manner as presented in [30]. In addition, we compared again the ST-SMC response with optimized PID to show the behaviour of QUAV with each algorithm. The results obtained from the simulation emphasise the ability of ST-SMC to contrast disturbances and demonstrate that the PID is difficult to operate under these conditions. Figure 7 shows the tridimensional performance of QUAV on path-following while a disturbance is applied. In Figure 7(a), we can observe the dynamic response when PID is implemented. The movements of QUAV present oscillation of a considerable magnitude. In contrast to PID response, ST-SMC can overcome the disturbance, maintaining a minimal tracking trajectory error in Figure 7(b).

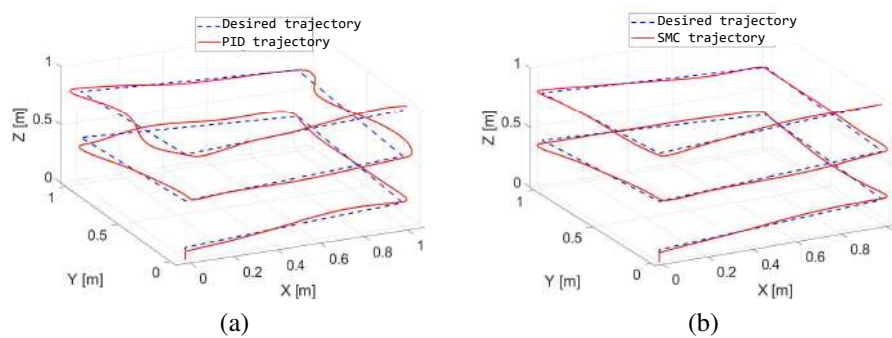| (a) | (b) |

Figure 7. Comparison of PID and ST-SMC controller tracking performance adding a disturbance (a) QUAV Performance on X axis and (b) QUAV Performance on Y axis

5.2. Experimental results

This section presents the experimental results obtained while applying the proposed structure: ST-SMC optimized using the HGS algorithm to track QUAV. Experiments were developed in a platform with the structure shown in Figure 8. The platform is composed of a motion capture system conformed by eighth Vicon® Bonita cameras, linked by ROS that permits to known position and the attitude of a Parrot® QUAV bebop 1 as shown in Figure 8(a). ROS is an operating system that allows us to create communication nodes through topics: it will enable publishers to send information and subscribers to receive or read data from the platform. We use four nodes: i) Vicon bridge, a publisher that permits access to the position and attitude of QUAV at all times; ii) Bebop driver, a subscriber who receives commands like land and take off as well as control signals calculated by the controller; iii) Joy node permit us to activate the control node through the joystick buttons; and iv) control node that links all the nodes and manages the system tasks to command the switch of the manual to the automatic mode as shown in Figure 8(b). Desired trajectories were the same as implemented in the simulation (section 5.1). Physical and gain parameters are shown in Tables 2 and 3 , where all the parameters are multiplied by $1/2300$ because the bebop QUAV allows signal control around $10e - 3$. That relation was found during the tests.

The performance in the experimentation was similar to that reported in the simulation results. The QUAV successfully tracked the desired trajectory in both tests with PID and ST-SMC algorithms when it had no disturbance. The similarity of tridimensional trajectory performance of both optimised algorithms can be observed in Figure 9. Translational dynamics X and Y suffer an overshoot and oscillation as a result of changes of direction in the desired trajectory, as we observed in both experiments: PID, Figure 9(a), and ST-SMC, Figure 9(b). The altitude dynamic presents a maximum error when the trajectory is started. That is a consequence of the rebound effect on the floor that diminishes as QUAV elevates. The similarity of tridimensional trajectory performance of both optimised algorithms in Figure 9 can be observed.
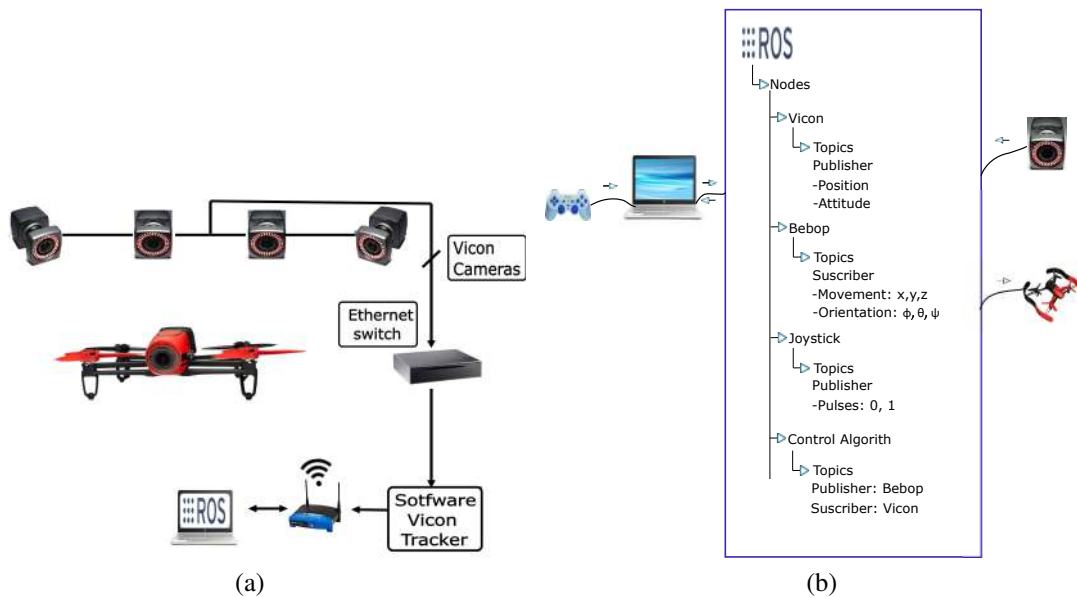

Figure 8. Structure of platform for the experimental tests (a) diagram of the experimental platform used to test the optimised controllers and (b) structure for communication applied in the experimental platform with ROS

In Figure 10, the results of the experiment are shown when a disturbance of $\frac{1}{2}\sin(t)$ was applied. Figure 10(a) shows the behavior of the dynamics in the axes $X - Y - Z$ when the PID algorithm is implemented. We can observe that the QUAV presents oscillations mainly in the translational dynamics. On the other hand, when the ST-SMC algorithm is implemented, the vehicle is maintained with a minimum error during trajectory tracking, demonstrating its robustness against disturbance as shown in Figure 10(b). Finally, data of the experiments carried out are available in https://github.com/nasamzp/Optimization-of-a-ST-SMC-control-for-path-tracking-3D-with-perturbations-of-a-QUAV-using-the-Huger-G.
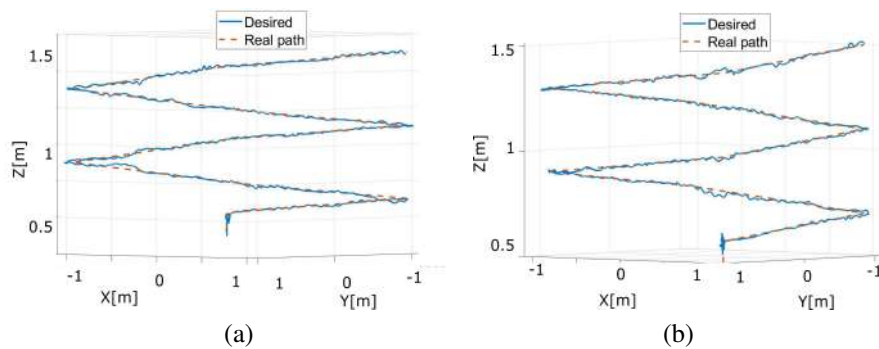
Figure 9. Experimental tracking performance of QUAV. The experiment developed without disturbance (a) QUAV Performance in X-Y-Z axes with PID controller and (b) QUAV Performance in X-Y-Z axes with ST-SMC controller
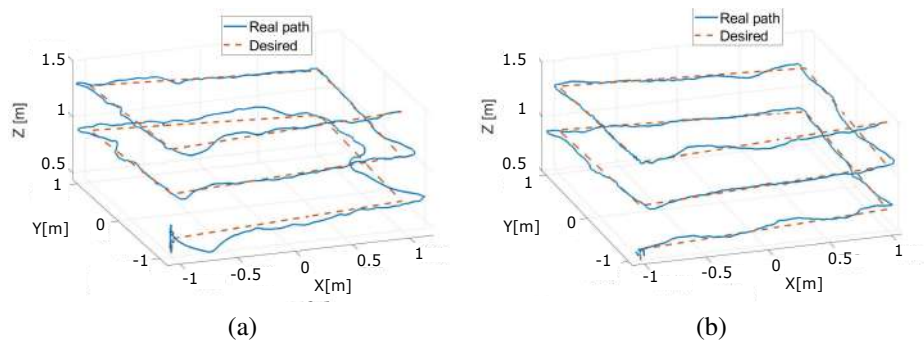

Figure 10. Performance comparison of PID and ST-SMC controllers applying a disturbance (a) experimental tracking performance of PID controller adding a disturbance and (b) experimental tracking performance of ST-SMC controller adding a disturbance

6.   CONCLUSION

This paper addresses the parameterisation problem of control for tridimensional tracking in the presence of disturbances of a QUAV vehicle, modelled with six dynamics. The proposed ST/SMC controller parameters were optimised, minimising the error between the desired trajectory and the actual using the HGS meta-heuristic algorithm. The performance of the ST-SMC controller is compared with a PID controller to validate robustness. The RMSE performance index was evaluated for both algorithms in simulations using Matlab and experimental results using a Vicon system platform. Numerical and experimental tests present likeness performance with ST-SMC carrying out the tracking task more effectively. Tests showed that the ST-SMC controller could overcome an applied disturbance while tracking the QUAV with a strong performance for all dynamics. The results obtained emphasise the ability of ST-SMC to contrast disturbances and demonstrate that the PID is difficult to operate under these conditions. The experimental results proved that the PID controller presented the most significant error with an RSME=0.0902, compared with RSME=0.0658 of ST-SMC. The stability of the dynamics is guaranteed, developing the stability analysis in the sense of Lyapunov for the parameters obtained by the HGS metaheuristic algorithm. Forthcoming works are implementing an optimised ST-SMC controller in QUAV with a payload system.

REFERENCES

[1]   S. N. Mohanty, J. V. R. Ravindra, G. S. Narayana, C. R. Pattnaik, and Y. M. Sirajudeen, *Eds., Drone technology: future trends and practical applications*, 1st ed. Wiley-Scrivener, 2023, pp. 37–110.

[2]   J.-S. Um, *Drones as cyber-physical systems.* Singapore: Springer, 2019, pp. 37-59. doi: 10.1007/978-981-13-3741-3.

[3]   M. A. Lotufo, L. Colangelo, C. Perez-Montenegro, E. Canuto, and C. Novara, "UAV quadrotor attitude control: An ADRC-EMC combined approach," *Control Engineering Practice*, vol. 84, pp. 13–22, Mar. 2019, doi: 10.1016/j.conengprac.2018.11.002.

[4]   S. Yu, X. Fan, J. Qi, L. Wan, and B. Liu, "Attitude control of quadrotor UAV based on integral backstepping active disturbance rejection control," *Transactions of the Institute of Measurement and Control*, Jul. 2023, doi: 10.1177/01423312231185423.

[5]   A. E. M. Redha, R. B. Abduljabbar, and M. S. Naghmash, "Drone altitude control using proportional integral derivative technique and recycled carbon fiber structure," in *Lecture Notes in Networks and Systems*, vol. 299, Springer International Publishing, 2022, pp. 55–67. doi: 10.1007/978-3-030-82616-1_6.

[6]   H. Bi, G. Qi, and J. Hu, "Modeling and analysis of chaos and bifurcations for the attitude system of a quadrotor unmanned aerial vehicle," *Complexity*, vol. 2019, pp. 1–16, Oct. 2019, doi: 10.1155/2019/6313925.

[7]   E. A. Chater, H. Housny, and H. El Fadil, "Adaptive proportional integral derivative deep feedforward network for quadrotor trajectory-tracking flight control," *International Journal of Electrical and Computer Engineering (IJECE)*, vol. 12, no. 4, pp. 3607–3619, Aug. 2022, doi: 10.11591/ijece.v12i4.pp3607-3619.

[8]   L. Cavanini, G. Ippoliti, and E. F. Camacho, "Model predictive control for a linear parameter varying model of an UAV," *Journal of Intelligent and Robotic Systems: Theory and Applications*, vol. 101, no. 3, pp. 1–18, Mar. 2021, doi: 10.1007/s10846-021-01337-x.

[9]   N. Koksal, H. An, and B. Fidan, "Backstepping-based adaptive control of a quadrotor UAV with guaranteed tracking performance," *ISA Transactions*, vol. 105, pp. 98–110, Oct. 2020, doi: 10.1016/j.isatra.2020.06.006.

[10]   M. A. M. Basri and A. Noordin, "Optimal backstepping control of quadrotor UAV using gravitational search optimization algorithm," *Bulletin of Electrical Engineering and Informatics*, vol. 9, no. 5, pp. 1819–1826, Oct. 2020, doi: 10.11591/eei.v9i5.2159.

[11]   V. Razmavar, H. A. Talebi, and F. Abdollahi, "A composite controller based on nonlinear H∞ and nonlinear disturbance observer for attitude stabilization of a flying robot," *Indonesian Journal of Electrical Engineering and Computer Science (IJEECS)*, vol. 22, no. 1, pp. 270–276, Apr. 2021, doi: 10.11591/ijeecs.v22.i1.pp270-276.

[12]   L. V. Nguyen, M. D. Phung, and Q. P. Ha, "Iterative learning sliding mode control for UAV trajectory tracking," *Electronics (Switzerland)*, vol. 10, no. 20, p. 2474, Oct. 2021, doi: 10.3390/electronics10202474.

[13]   T. Huang, D. Huang, Z. Wang, and A. Shah, "Robust tracking control of a quadrotor UAV based on adaptive sliding mode controller," *Complexity*, vol. 2019, pp. 1–15, Dec. 2019, doi: 10.1155/2019/7931632.

[14]   Y. Mehmood, J. Aslam, N. Ullah, M. S. Chowdhury, K. Techato, and A. N. Alzaed, "Adaptive robust trajectory tracking control of multiple quad-rotor UAVs with parametric uncertainties and disturbances," *Sensors*, vol. 21, no. 7, p. 2401, Mar. 2021, doi: 10.3390/s21072401.

[15]   Y. Shtessel, C. Edwards, L. Fridman, and A. Levant, *Sliding mode control and observation.* Springer New York, 2014. doi: 10.1007/978-0-8176-4893-0.

[16]   F. Muñoz, E. S. Espinoza, I. González-Hernández, S. Salazar, and R. Lozano, "Robust trajectory tracking for unmanned aircraft systems using a nonsingular terminal modified super-twisting sliding mode controller," *Journal of Intelligent and Robotic Systems: Theory and Applications*, vol. 93, no. 1–2, pp. 55–72, Jun. 2019, doi: 10.1007/s10846-018-0880-y.

[17]   L. Cui, R. Zhang, H. Yang, and Z. Zuo, "Adaptive super-twisting trajectory tracking control for an unmanned aerial vehicle under gust winds," *Aerospace Science and Technology*, vol. 115, p. 106833, Aug. 2021, doi: 10.1016/j.ast.2021.106833.

[18]   S. Garcia-Nava et al., "Development of a 6 degree of freedom unmanned underwater vehicle: design, construction and real-time experiments," *Journal of Marine Science and Engineering*, vol. 11, no. 9, p. 1744, Sep. 2023, doi: 10.3390/jmse11091744.

[19]   A. Q. Al-Dujaili, A. Falah, A. J. Humaidi, D. A. Pereira, and I. K. Ibraheem, "Optimal super-twisting sliding mode control design of robot manipulator: design and comparison study," *International Journal of Advanced Robotic Systems*, vol. 17, no. 6, p. 1–17, Nov. 2020, doi: 10.1177/1729881420981524.

[20]   V. Utkin, A. Poznyak, Y. Orlov, and A. Polyakov, "Conventional and high order sliding mode control," *Journal of the Franklin Institute*, vol. 357, no. 15, pp. 10244–10261, Oct. 2020, doi: 10.1016/j.jfranklin.2020.06.018.

[21]   H. Moayedi, M. Mehrabi, D. T. Bui, B. Pradhan, and L. K. Foong, "Fuzzy-metaheuristic ensembles for spatial assessment of forest fire susceptibility," *Journal of Environmental Management*, vol. 260, p. 109867, Apr. 2020, doi: 10.1016/j.jenvman.2019.109867.

[22]   M. A. Ebrahim, M. N. Ahmed, H. S. Ramadan, M. Becherif, and J. Zhao, "Optimal metaheuristic-based sliding mode control of VSC-HVDC transmission systems," *Mathematics and Computers in Simulation*, vol. 179, pp. 178–193, Jan. 2021, doi: 10.1016/j.matcom.2020.08.009.

[23]   W. Boukadida, A. Benamor, H. Messaoud, and P. Siarry, "Metaheuristics-based multi-objective design of global robust optimal sliding mode control of discrete uncertain systems," *International Journal of Control, Automation and Systems*, vol. 17, no. 6, pp. 1378–1392, May 2019, doi: 10.1007/s12555-018-0486-y.

[24]   M. Zare, F. Pazooki, and S. E. Haghighi, "Quadrotor UAV position and altitude tracking using an optimized fuzzy-sliding mode control," *IETE Journal of Research*, vol. 68, no. 6, pp. 4406–4420, Jul. 2022, doi: 10.1080/03772063.2020.1793694.

[25]   A. Mughees and I. Ahmad, "Multi-optimization of novel conditioned adaptive barrier function integral terminal SMC for trajectory tracking of a quadcopter system," *IEEE Access*, vol. 11, pp. 88359–88377, 2023, doi: 10.1109/ACCESS.2023.3304760.

[26]   N. S. Zuñiga-Peña, N. Hernández-Romero, J. C. Seck-Tuoh-mora, J. Medina-Marin, and I. Barragan-Vite, "Improving 3D path tracking of unmanned aerial vehicles through optimization of compensated PD and PID controllers," *Applied Sciences (Switzerland)*, vol. 12, no. 1, p. 99, Dec. 2022, doi: 10.3390/app12010099.

[27]   H. Khalil, *Nonlinear Control*, 1st ed. England: Pearson Education, 2015.

[28]   H. Hamadi, B. Lussier, I. Fantoni, C. Francis, and H. Shraim, "Observer-based super twisting controller robust to wind perturbation for multirotor UAV," in *2019 International Conference on Unmanned Aircraft Systems, ICUAS 2019*, Jun. 2019, pp. 397–405, doi: 10.1109/ICUAS.2019.8798307.

[29]   Y. Yang, H. Chen, A. A. Heidari, and A. H. Gandomi, "Hunger games search: visions, conception, implementation, deep analysis, perspectives, and towards performance shifts," *Expert Systems with Applications*, vol. 177, p. 114864, Sep. 2021, doi: 10.1016/j.eswa.2021.114864.

[30] F. Muñoz, I. González-Hernández, S. Salazar, E. S. Espinoza, and R. Lozano, "Second order sliding mode controllers for altitude control of a quadrotor UAS: Real-time implementation in outdoor environments," *Neurocomputing*, vol. 233, pp. 61–71, Apr. 2017, doi: 10.1016/j.neucom.2016.08.111.
[31] J. E. Velázquez-Velázquez, V. L. Kharitonov, and S. Mondié, "Robust stability analysis of a class of neutral type time delay equations," in *Proceedings of the IEEE Conference on Decision and Control*, 2008, pp. 4646–4651, doi: 10.1109/CDC.2008.4738807.
[32] S. Sun, R. J. Schilder, and C. C. De Visser, "Identification of quadrotor aerodynamic model from high speed flight data," *AIAA Atmospheric Flight Mechanics Conference, 2018*, Jan. 2018, doi: 10.2514/6.2018-0523.

BIOGRAPHIES OF AUTHORS

Nadia Samantha Zuñiga-Peña received his M.S. degree in mechatronics from the Polytechnic University of Pachuca in 2018. She was a lecturer at the same university until 2020. She is a Ph.D. student and a lecturer at the University of Hidalgo State, Pachuca, Hidalgo, Mexico. Her main research interest is intelligent control and optimization techniques applied to mechatronics systems and UAVs. She can be contacted at email: nadia_zuniga@uaeh.edu.mx.

Norberto Hernández-Romero received the M.S. degree from the Department of Electrical Engineering, Laguna Technological Institute, Mexico, in 2001, and the Ph.D. degree from the Autonomous University of Hidalgo State, Pachuca, Hidalgo, Mexico, in 2009. He is currently a Professor with the Advanced Research in Industrial Engineering Centre, Autonomous University of Hidalgo State. He is also a member of the national system of researchers (SNI), where he is currently level 1. His current research interests include system identification, feedback control design, genetic algorithms, fuzzy logic, neural networks, and its applications. He can be contacted at email: nhromero@uaeh.edu.mx.

Juan Carlos Seck-Tuoh-Mora received the M.S. and Ph.D. degrees in Computer Science from the Center for Research and Advanced Studies, National Polytechnic Institute, Mexico, in 1999 and 2002, respectively. He is currently a Professor-Researcher in the academic area of engineering with the Autonomous University of the State of Hidalgo. He is also a national researcher level 2 within the national system of researchers of CONACYT. His current research interests include cellular automata, metaheuristics, evolutionary algorithms, and neural networks to model, design, optimize, and control engineering systems. He can be contacted at email: jseck@uaeh.edu.mx.

Joselito Medina-Marin received the M.S.and Ph.D. degrees in Electrical Engineering from the Research and Advanced Studies Centre, National Polytechnic Institute, Mexico, in 2002 and 2005, respectively. He is currently a Professor with the Advanced Research in Industrial Engineering Centre, Autonomous University of Hidalgo State, Pachuca, Hidalgo, Mexico. He is also a member of the National System of Researchers (SNI), where he is currently level 1. His current research interests include artificial neural networks, petri net theory and its applications, active databases, simulation, and programming languages. He can be contacted at email: jmedina@uaeh.edu.mx.

Julio Cesar Ramos-Fernández received a Ph.D. in Computational Sciences in Mexico and Ph.D. Engineering and Applied Science in France in 2008. He is a professor at Polytechnic University of Pachuca in the mechatronics department since 2008, and he is the technical head of the National Laboratory in Autonomous Vehicles and Exoskeletons of the PUP campus by the National Council of Science and Technology of Mexico(CONACYT). His research interests lie in the area of mechatronics systems, fuzzy logic modelling and control, applied to precision agriculture. He can be contacted at email: jramos@upp.edu.mx.